

SCIENTIFIC REPORTS



OPEN

Oxidative Stress and Immune Responses During Hepatitis C Virus Infection in *Tupaia belangeri*

Mohammad Enamul Hoque Kayesh^{1,2}, Sayeh Ezzikouri^{3,4}, Takahiro Sanada⁵, Haiying Chi^{2,3}, Yukiko Hayashi⁶, Khadija Rebbani^{2,3}, Bouchra Kitab^{2,3}, Aya Matsuu^{2,3}, Noriaki Miyoshi⁷, Tsunekazu Hishima⁶, Michinori Kohara⁵ & Kyoko Tsukiyama-Kohara^{1,2,3}

Hepatitis C virus (HCV) is a leading cause of chronic liver disease, cirrhosis, and hepatocellular carcinoma. To address the molecular basis of HCV pathogenesis using tupaia (*Tupaia belangeri*), we characterized host responses upon HCV infection. Adult tupaia were infected with HCV genotypes 1a, 1b, 2a, or 4a. Viral RNA, alanine aminotransferase, anti-HCV core and anti-nonstructural protein NS3 antibody titres, reactive oxygen species (ROS), and anti-3 β -hydroxysterol- Δ 24reductase (DHCR24) antibody levels were measured at 2-week intervals from 0 to 41 weeks postinfection. All HCV genotypes established infections and showed intermittent HCV propagation. Moreover, all tupaia produced anti-core and anti-NS3 antibodies. ROS levels in sera and livers were significantly increased, resulting in induction of DHCR24 antibody production. Similarly, lymphocytic infiltration, disturbance of hepatic cords, and initiation of fibrosis were observed in livers from HCV-infected tupaia. Intrahepatic levels of Toll-like receptors 3, 7, and 8 were significantly increased in all HCV-infected tupaia. However, interferon- β was only significantly upregulated in HCV1a- and HCV2a-infected tupaia, accompanied by downregulation of sodium taurocholate cotransporting polypeptide. Thus, our findings showed that humoral and innate immune responses to HCV infection, ROS induction, and subsequent increases in DHCR24 auto-antibody production occurred in our tupaia model, providing novel insights into understanding HCV pathogenesis.

Hepatitis C virus (HCV) is a major public health problem that infects approximately 130–170 million people worldwide^{1,2}. HCV causes chronic hepatitis and is a major cause of liver cirrhosis and hepatocellular carcinoma (HCC)¹. The first line of immune defence against HCV relies on cell-intrinsic innate immunity within hepatocytes. The HCV genome is a single-stranded, positive-sense RNA genome. During viral replication, HCV is sensed as non-self by pattern recognition receptors (PRRs) in the host cell, which identify and bind to pathogen-associated molecular patterns (PAMPs) within viral products, leading to activation of innate and adaptive immune responses³. Both effective innate and adaptive immune responses are involved in the control of HCV infections⁴; however, the role of the humoral immune system in HCV clearance is still unclear⁵.

Toll-like receptors (TLRs), an important component of innate immunity, play crucial roles in sensing invaders and initiating innate immune responses, thereby limiting the spreading of infections and modulating adaptive immune responses⁶. Sodium taurocholate cotransporting polypeptide (NTCP), a bile acid transporter expressed at the hepatocyte basolateral membrane⁷, can act as a regulator of antiviral immunity in HCV infection⁸. HCV infection can induce reactive oxygen species (ROS) production^{9,10} and oxidative stress can lead to the formation

¹Department of Pathological and Preventive Veterinary Science, The United Graduate School of Veterinary Science, Yamaguchi University, Yamaguchi, Japan. ²Laboratory of Animal Hygiene, Joint Faculty of Veterinary Medicine, Kagoshima University, Kagoshima, Japan. ³Transboundary Animal Diseases Centre, Joint Faculty of Veterinary Medicine, Kagoshima University, Kagoshima, Japan. ⁴Virology Unit, Viral Hepatitis Laboratory, Institut Pasteur du Maroc, Casablanca, Morocco. ⁵Department of Microbiology and Cell Biology, Tokyo Metropolitan Institute of Medical Science, Tokyo, Japan. ⁶Department of Pathology, Tokyo Metropolitan Komagome Hospital, Bunkyo-ku, Tokyo, Japan. ⁷Department of Animal Pathology, Joint Faculty of Veterinary Medicine, Kagoshima University, Kagoshima, Japan. Mohammad Enamul Hoque Kayesh and Sayeh Ezzikouri contributed equally to this work. Correspondence and requests for materials should be addressed to M.K. (email: kohara-mc@igakuken.or.jp) or K.T.-K. (email: kkohara@vet.kagoshima-u.ac.jp)

of 8-hydroxydeoxyguanosine (8-OHdG), an indicator of oxidative DNA damage¹¹. 3 β -Hydroxysterol- Δ 24reductase (DHCR24), a cholesterol biosynthetic enzyme¹², is an essential host factor that plays a significant role in HCV replication¹³. Moreover, anti-DHCR24 auto-antibody levels are increased during the progression of HCV infection¹⁴. Indeed, the detection rate of HCC by anti-DHCR24 antibodies is higher (70.6%) than that of the standard HCC markers, alpha-fetoprotein (54.8%) or protein induced by vitamin K absence or antagonist-II (42.5%)¹⁴.

Recently, HCV can be completely cured by newly approved drugs, direct-acting antivirals (DAAs)^{15, 16}. However, persistent hepatic inflammation, cirrhosis, and HCC have been reported in patients following viral clearance¹⁷. To solve these issues and develop an efficient vaccine against HCV, animal models are essential. Lack of small animal models is a great obstacle in the field of HCV research. To date, chimpanzees have been used as infection models for HCV. However, high costs and ethical concerns have restricted the use of chimpanzees in experimental infections. Recently, humanized chimeric mice¹⁸ and genetically humanized mice¹⁹ have been developed for use in HCV infection models^{13, 18}. However, the use of mice has some disadvantages, including high cost, immunocompromised animal status, donor-to-donor variability, and inability to examine chronic infections. *Tupaia belangeri* belongs to the *Tupaiaidae* family, which contains four genera and 19 extant species²⁰. The evolutionary characterization of 7 S RNA-derived short interspersed elements (SINEs) has shown that tupaia possess specific, chimeric Tu type II SINEs and can be clustered with primates²¹. Thus, genomic analysis suggested that tupaia are more closely related to humans than to rodents^{21, 22}. Tupaia have been reported to be susceptible to several hepatotropic viruses that also infect humans, including hepatitis B virus^{23, 24}, HCV^{25, 26}, and hepatitis E virus²⁷, and can be developed as an immunocompetent animal infection model. However, the molecular basis of HCV pathogenesis has not been fully characterized in the tupaia model due to a lack of characterization tools (e.g., specific antibodies, quantitative polymerase chain reaction [qPCR] assays, and cDNAs).

Therefore, in this study, we evaluated the susceptibility of tupaia to several viral strains of HCV and characterized the effects of HCV infection on ROS generation and its association with anti-DHCR24 antibody levels. We also characterized humoral immune responses to viral proteins and established a qPCR assay to evaluate TLR, NTCP, and cytokine expression to characterize the innate immune response during HCV infection, which may provide significant insight into HCV pathogenesis.

Results

Alanine aminotransferase (ALT) levels and viral loads in HCV-infected tupaia sera. Tupaia were infected with HCV genotypes 1a (#21), 1b (#22), 4a (#23), and 2a (#24). The level of ALT fluctuated, and intermittent growth of HCV was observed in all tupaia (Figs 1A, 2A, 3A and 4A). The highest ALT level (317.5 IU/L) was observed in tupaia #23 at 29 weeks postinfection (wpi). Virus could be detected in serum at 25 (51 copies/mL) and 31 wpi (43 copies/mL) in tupaia #21; at 13 wpi (21 copies/mL) in tupaia #22; at 7 (4 copies/mL), 29 (13 copies/mL), and 31 wpi (50 copies/mL) in tupaia #23; and at 11 (120 copies/mL), 15 (2 copies/mL), and 23 wpi (75 copies/mL) in tupaia #24 (Figs 1A, 2A, 3A and 4A).

Measurement of anti-core and anti-NS3 antibody titres. To investigate the course of HCV-specific humoral immune responses in HCV-infected tupaia, we measured the levels of anti-core and anti-NS3 antibody titres in serum samples before infection (0 wpi) and every 2 weeks from 3 wpi to until the tupaia were sacrificed at 41 wpi. Despite fluctuations, significant increases in anti-core antibody levels were observed in all tupaia from 3 to 41 wpi (Figs 1B, 2B, 3B and 4B). In tupaia #21, significant increases in anti-NS3 antibody titres were observed at 3 and 25–35 wpi (Fig. 1B). In tupaia #22, significant increases in anti-NS3 antibody titres were observed at 3, 15, and 21–41 wpi (Fig. 2B). Significant increases in anti-NS3 antibodies were observed in tupaia #23 and #24 from 3 to 41 wpi (Figs 3B and 4B).

At 3 wpi, though virus could not be detected in sera, a significant increase in anti-core and anti-NS3 antibody production was observed in all HCV-infected tupaia. Anti-core antibody production was decreased after the initial increase at 3 wpi, which further increased during or around peak viral propagation and fluctuated (Figs 1B, 2B, 3B and 4B). The highest anti-core antibody production was observed in tupaia #22 at 29 wpi (Fig. 2B). Additionally, anti-NS3 antibody production sharply decreased after 3 wpi and fluctuated. The highest anti-NS3 antibody production was observed in tupaia #23 at 3 wpi (Fig. 3B). Overall, peak NS3 antibody production was observed during or after peak viral propagation. Anti-core and anti-NS3 antibody titres in uninfected controls and positive controls were measured to ensure the specificity of the assay (Fig. S1A,B).

Histological analysis of liver tissues from HCV-infected tupaia. Histological analysis showed chronic hepatitis including abnormal architecture of liver cell cords, piecemeal necrosis, hepatocyte swelling, and lymphocytic infiltration into liver tissues of HCV-infected tupaia compared with that of normal tupaia liver tissues (Fig. 5). Silver staining showed increased fibres among hepatocytes (tupaia #21 and #22) (Fig. 5C, D) and thickened fibres (tupaia #23 and #24) (Fig. 5E, F), indicating the progression of fibrosis in HCV-infected tupaia livers.

Measurement of ROS levels and anti-DHCR24 antibody titres. To investigate the effects of HCV infection on ROS generation, we measured ROS levels in sera from HCV-infected tupaia at 2-week intervals from 0 to 41 wpi. ROS levels were increased in all HCV-infected tupaia compared to ROS levels before infection (Figs 1C, 2C, 3C and 4C). ROS levels were also evaluated in mock-infected controls and with different concentrations of H₂O₂ as a positive control to ensure the appropriateness of the assay conditions (Fig. S1C).

To investigate whether increased ROS production induced anti-DHCR24 auto-antibody levels in HCV-infected tupaia, we measured the levels of serum anti-DHCR24 antibodies at 2-week intervals from 0 to 41 wpi. High levels of serum anti-DHCR24 antibodies were observed in all HCV-infected tupaia following ROS

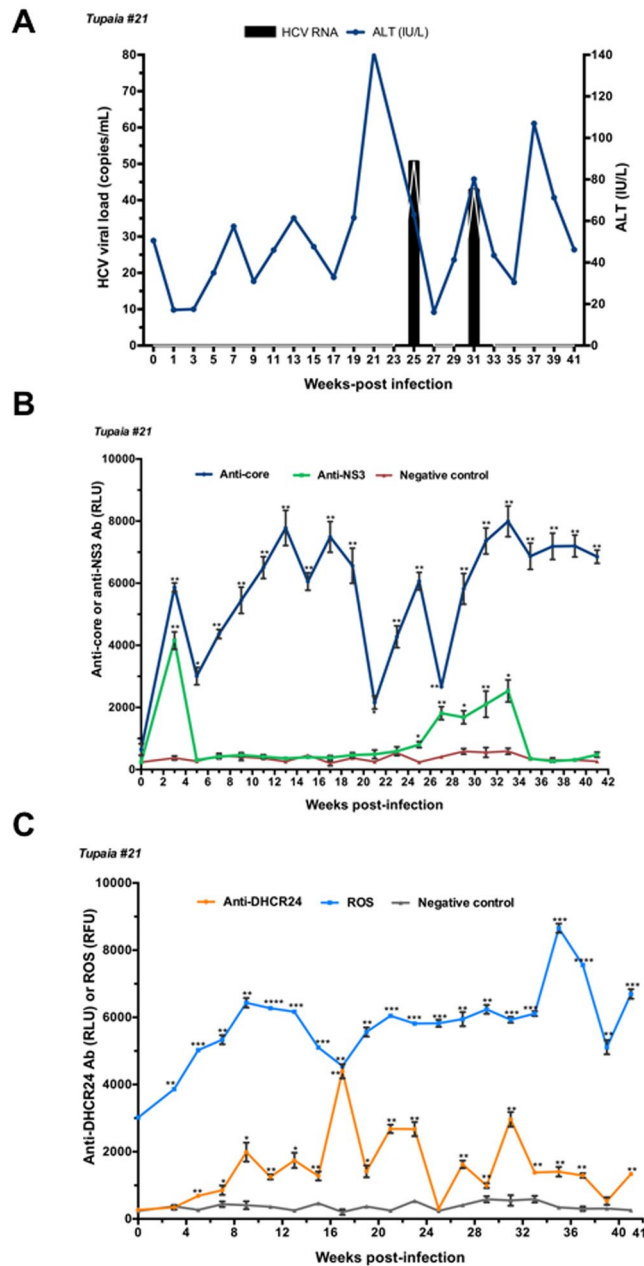


Figure 1. Response of tupaia #21 to HCV1a infection. **(A)** ALT levels and viral loads in sera from tupaia #21 collected at 2-week intervals from 0 to 41 weeks postinfection (wpi). **(B)** Anti-HCV core and anti-nonstructural protein NS3 antibody titres in tupaia #21 at 2-week intervals from 0 to 41 wpi. **(C)** Anti-DHCR24 antibody titres and ROS levels in tupaia #21 at 2-week intervals from 0 to 41 wpi. The empty vector was used as the negative control. * $p < 0.05$, ** $p < 0.01$, *** $p < 0.001$, and **** $p < 0.0001$ indicate significant differences in antibody titres or ROS levels, as appropriate, before infection and after infection at different weeks. Data are presented as means \pm SDs ($n = 2$).

induction (Figs 1C, 2C, 3C and 4C). To ensure the specificity of the assay, anti-DHCR24 antibody titres in normal and positive controls were also evaluated (Fig. S1D).

Measurement of oxidative stress in the liver. To determine intrahepatic oxidative stress, we measured ROS levels in liver tissues at 41 wpi in normal and HCV-infected tupaia and found significantly higher ROS levels in HCV-infected tupaia liver tissues compared to normal controls (Fig. 6A). Additionally, at 41 wpi, we measured 8-OHdG levels in genomic DNA extracted from HCV-infected tupaia liver tissues to evaluate oxidative DNA damage. A significant increase in 8-OHdG levels was observed in all HCV-infected tupaia compared to normal controls (Fig. 6B).

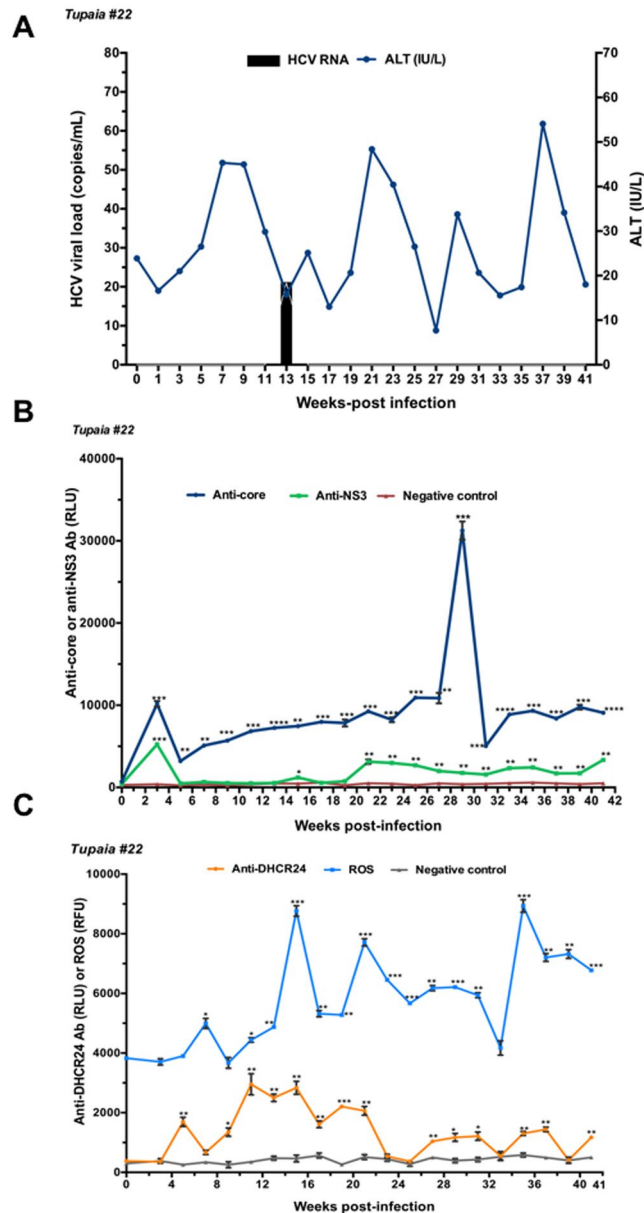


Figure 2. Response of tupaia #22 to HCV1b infection. **(A)** ALT levels and viral loads in sera from tupaia #22 collected at 2-week intervals from 0 to 41 weeks postinfection (wpi). **(B)** Anti-HCV core and anti-nonstructural protein NS3 antibody titres in tupaia #22 at 2-week intervals from 0 to 41 wpi. **(C)** Anti-DHCR24 antibody titres and ROS levels in tupaia #22 at 2-week intervals from 0 to 41 wpi. The empty vector was used as the negative control. * $p < 0.05$, ** $p < 0.01$, *** $p < 0.001$, and **** $p < 0.0001$ indicate significant differences in antibody titres or ROS levels, as appropriate, before infection and after infection at different weeks. Data are presented as means \pm SDs ($n = 2$).

Changes in TLR, NTCP, and cytokine expression in liver tissues. To investigate the mRNA expression patterns of TLRs, NTCP, and cytokines in liver tissues from HCV-infected tupaia, we isolated RNA from the livers of HCV-infected tupaia and measured the level of *TLR3*, *TLR7*, *TLR8*, *NTCP*, and cytokines (*interferon [IFN]- β* and *interleukin [IL]-6*) mRNAs at 41 wpi. Upregulation of *TLR3*, *TLR7*, and *TLR8* was observed in the liver tissues of all HCV-infected tupaia (#21, #22, #23, and #24) compared to uninfected normal tupaia (#3, #5, and #38; Fig. 7). *NTCP* was significantly suppressed in tupaia #21 and #24 and significantly upregulated in tupaia #22 and #23 (Fig. 8A). Moreover, significant upregulation of *IFN- β* was observed in all tupaia, except tupaia #22 (Fig. 8B). *IL-6* levels were significantly increased in tupaia #22 and #24 (Fig. 8C).

Discussion

In this study, we demonstrated, for the first time, that ROS levels were higher in sera and liver tissues from HCV-infected tupaia than in that from uninfected tupaia. These data were consistent with previous findings of higher ROS levels in sera²⁸ and liver tissues^{29,30} of HCV-infected patients. We also observed increased 8-OHdG

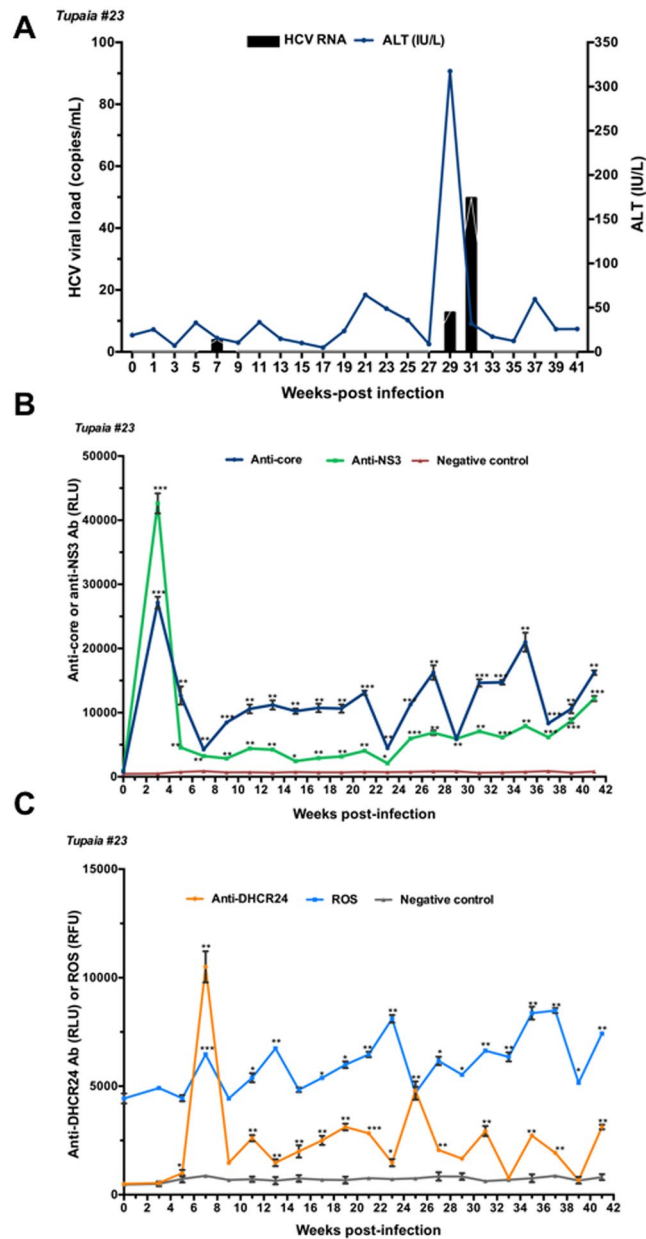


Figure 3. Response of tupaia #23 to HCV4a infection. (A) ALT levels and viral loads in sera from tupaia #23 collected at 2-week intervals from 0 to 41 weeks postinfection (wpi). (B) Anti-HCV core and anti-nonstructural protein NS3 antibody titres in tupaia #23 at 2-week intervals from 0 to 41 wpi. (C) Anti-DHCR24 antibody titres and ROS levels in tupaia #23 at 2-week intervals from 0 to 41 wpi. The empty vector was used as the negative control. * $p < 0.05$, ** $p < 0.01$, and *** $p < 0.001$ indicate significant differences in antibody titres or ROS levels, as appropriate, before infection and after infection at different weeks. Data are presented as means \pm SDs ($n = 2$).

levels in livers from HCV-infected tupaia. These data were consistent with previous findings of higher 8-OHdG levels in livers from patients with chronic HCV infections^{31,32}. Previous studies have found that ROS induces the upregulation of DHCR24^{10,33}. Consistent with these results, we showed that anti-DHCR24 antibody production was increased with ROS generation during the course of HCV infection in tupaia. Thus, the tupaia HCV infection model supported the possibility that anti-DHCR24 antibodies could be a valuable marker to monitor HCV infection *in vivo* and should be consistent with previous evidence demonstrating that anti-DHCR24 auto-antibodies could be a useful biomarker for hepatitis C progression¹⁴.

In this study, we also characterized humoral and intrahepatic innate immune responses in tupaia infected with different HCV strains. Anti-NS3 and anti-core antibodies have been reported to be predominant in chronic HCV infections³⁴. In fact, at 3 wpi, we found that all infected tupaia produced anti-core and anti-NS3 antibodies but were negative for serum HCV RNA. In our previous study, we detected HCV RNA only in the liver after 172 wpi²⁶; therefore, HCV may replicate in the liver but not be released into the serum via an unknown mechanism. A longitudinal study in humans, with a median follow-up of 7 years, also reported cases in which core antibody

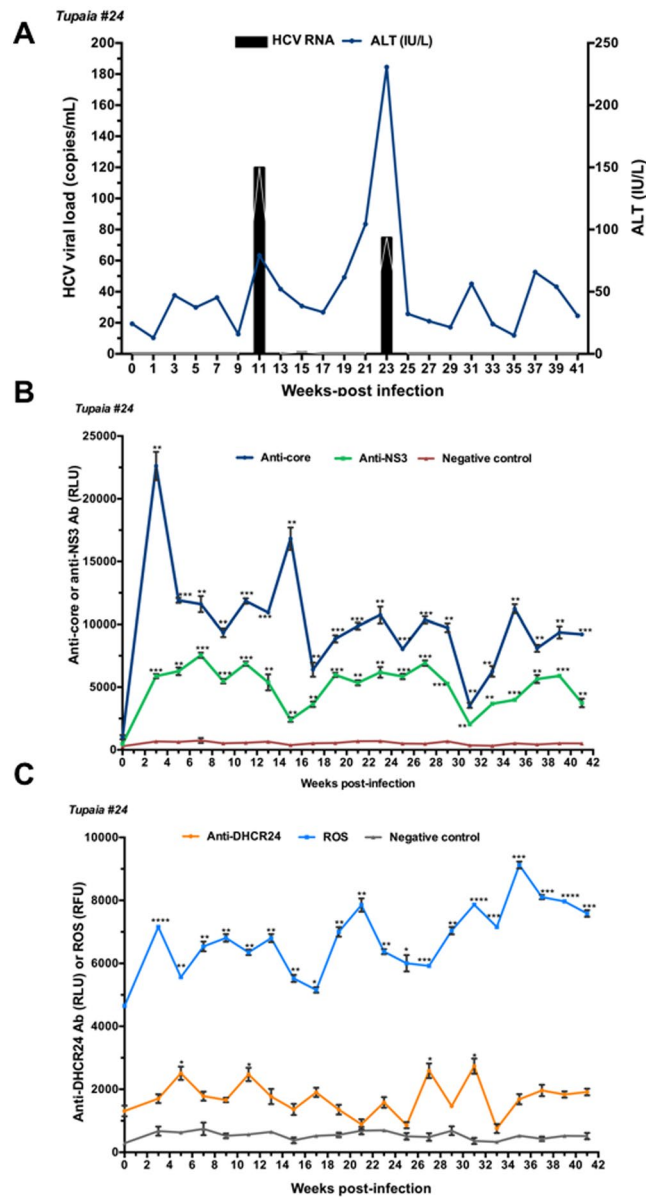


Figure 4. Response of tupaia #24 to HCV2a infection. **(A)** ALT levels and viral loads in sera from tupaia #24 collected at 2-week intervals from 0 to 41 weeks postinfection (wpi). **(B)** Anti-HCV core and anti-nonstructural protein NS3 antibody titres in tupaia #24 at 2-week intervals from 0 to 41 wpi. **(C)** Anti-DHCR24 antibody titres and ROS levels in tupaia #24 at 2-week intervals from 0 to 41 wpi. The empty vector was used as the negative control. * $p < 0.05$, ** $p < 0.01$, *** $p < 0.001$, and **** $p < 0.0001$ indicate significant differences in antibody titres or ROS levels, as appropriate, before infection and after infection at different weeks. Data are presented as means \pm SDs ($n = 2$).

was positive but HCV RNA was negative³⁵. Additionally, the highest anti-core antibody levels in tupaia #22 were observed at 29 wpi, indicating robust viral replication occurred somewhere in the tupaia body. At 41 wpi, upon histological analysis of liver tissues of HCV-infected tupaia, lymphocytic infiltration was observed, indicating the occurrence of inflammation in the liver.

TLRs are important initiators of cytokine production, and the TLR signalling pathway serves as a link between innate and acquired immunity^{36,37}. TLRs act as PRRs for recognizing HCV PAMPs³⁸. In our study, we found significant increases in *TLR3*, *TLR7*, and *TLR8* mRNA levels in liver tissues in chronically HCV-infected tupaia with different genotypes. Our results highlighted that HCV could trigger innate immune responses in livers of chronically infected tupaia. Thus, our data confirmed previous studies reporting that HCV could be recognized by TLR3, TLR7, and TLR8 in cell cultures^{39,40}.

HCV mainly infects hepatocytes, and two PRRs (retinoic acid-inducible genes I [RIG-I] and TLR3) recognize HCV RNA to trigger production of multiple cytokines, including type I IFN. HCV develops strategies to evade these immune responses through several mechanisms; for example, the cleavage or relocalisation of IFN- β

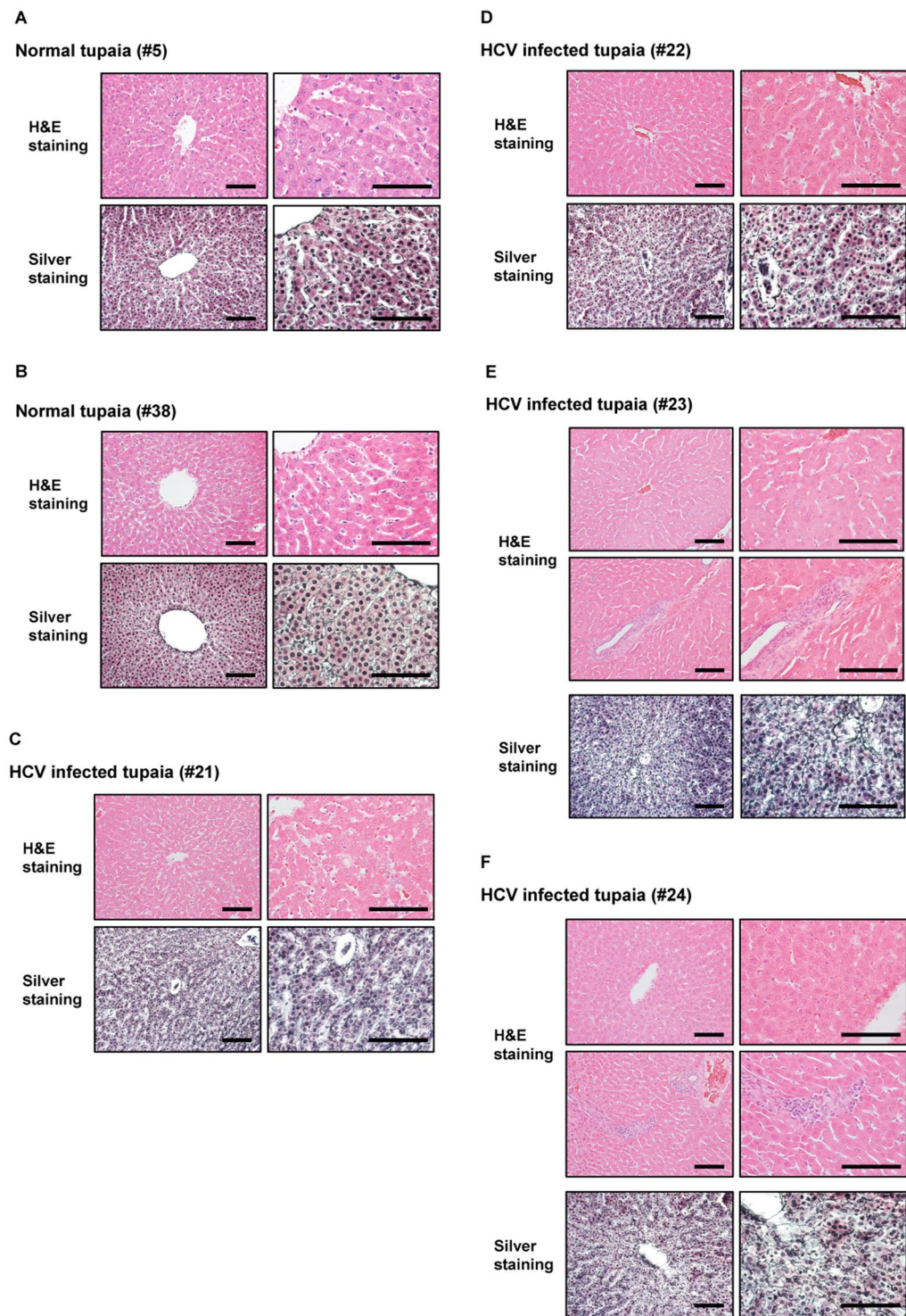


Figure 5. Histopathological analysis of liver tissues from normal and HCV-infected tupaia at 41 wpi. Histopathological analysis was performed with H&E or silver staining. H&E staining images (upper panel) and silver staining images (lower panel) of liver tissues from (A) Normal tupaia #5, (B) Normal tupaia #38, (C) HCV genotype 1a-infected tupaia #21, (D) HCV genotype 1b-infected tupaia #22, (E) HCV genotype 4a-infected tupaia #23, and (F) HCV genotype 2a-infected tupaia #24 have been shown. Black bars indicate 100 μ m.

promoter stimulator 1 by HCV NS3/4A protease inhibits RIG-I signalling^{41–43}. Furthermore, NS3/4A disrupts the TLR3 pathway by degradation of TIR-domain-containing adapter-inducing IFN- β ⁴³. HCV core inhibits IFN signalling by interfering with the Janus kinase/signal transducer and activator of transcription pathway⁴⁴, and HCV NS5A blocks 2'5' oligoadenylate synthetase and induces IL-8^{45,46}. In livers from HCV-infected tupaia,

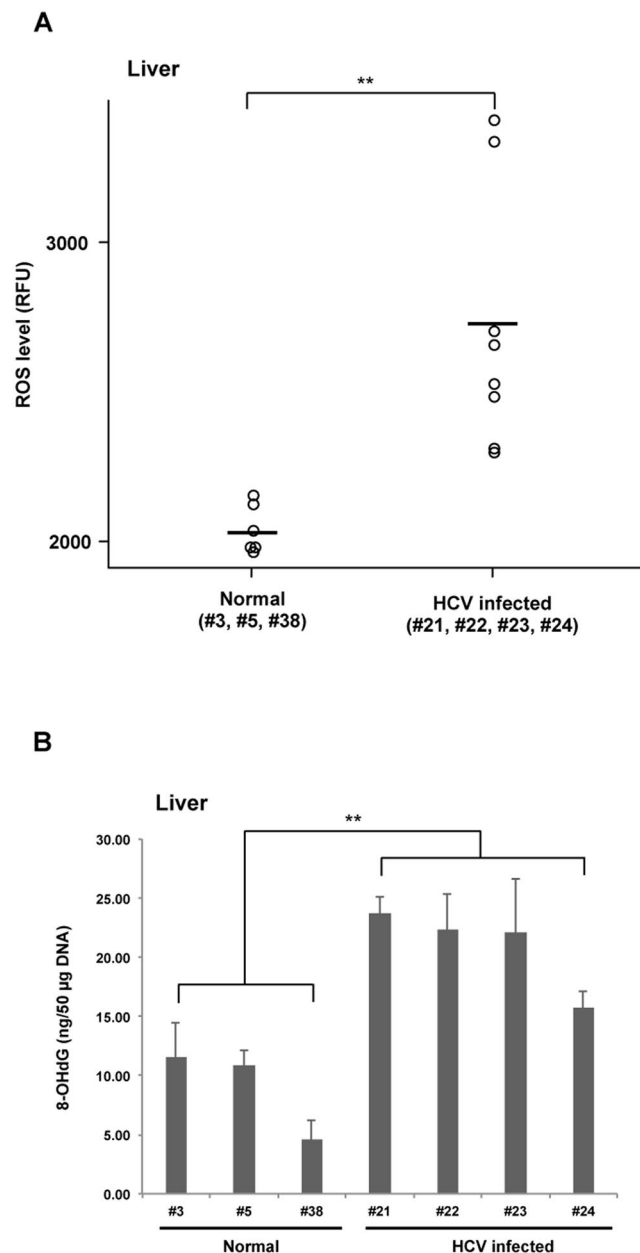


Figure 6. Intrahepatic ROS and 8-OHdG levels in normal and HCV-infected tupaia at 41 wpi. **(A)** ROS in liver lysates and **(B)** 8-OHdG levels in genomic DNA from HCV-infected tupaia were compared to those of normal controls. Horizontal bars in **(A)** indicate the mean value. ** $p < 0.01$ indicates significant differences compared to normal controls.

TLR3 was induced in all four tupaia, whereas downstream IFN- β induction was observed in three tupaia (#21, #23, and #24).

Silencing of NTCP could inhibit HCV infection, whereas overexpression of NTCP could enhance HCV infection in cell culture⁸. NTCP can act as a regulator of antiviral immune responses in the liver. Moreover, NTCP is associated with the IFN response, and increased NTCP expression could suppress interferon-induced transmembrane protein (IFITM)-2 and IFITM-3 expression, and vice versa⁸. In our study, we found downregulation of NTCP but upregulation of IFN- β in tupaia #21 and #24. Significant upregulation of NTCP was observed in tupaia #22 and #23, and upregulation of IFN- β was only observed in tupaia #23. Thus, further studies are needed to explore the detailed mechanisms involved in NTCP-IFN interactions in HCV infection.

In conclusion, the tupaia infection model developed in this study was an effective approach to analyse the pathogenesis of HCV infection. ROS generation induced by HCV infection may be a trigger for the generation of anti-DHCR24 antibodies. Production of anti-core and anti-NS3 antibodies and intrahepatic innate immune responses upon HCV infection by alterations of TLR, NTCP, and cytokine expression highlights the potential applications of the tupaia infection model for the evaluation of HCV pathogenesis. Furthermore, tupaia could be

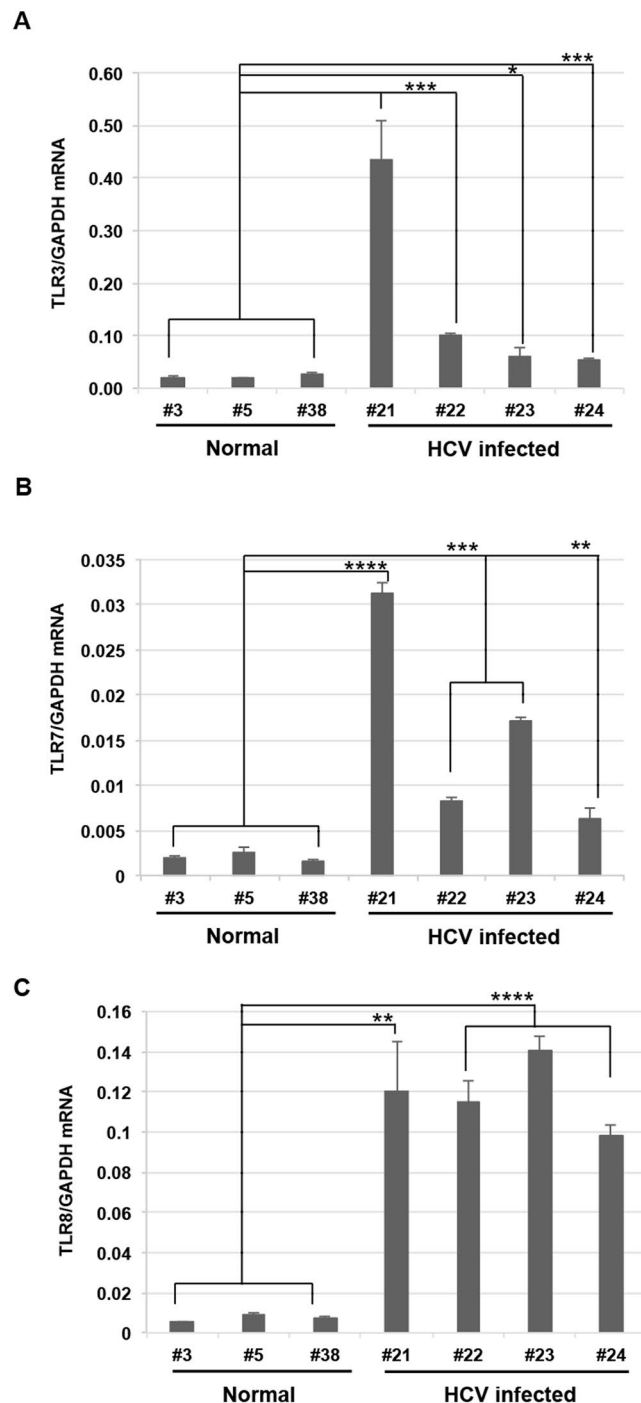


Figure 7. Changes in the expression of *TLR* mRNAs in HCV-infected tupaia at 41 wpi. (A) *TLR3*, (B) *TLR7*, and (C) *TLR8* mRNA expression in livers of HCV-infected tupaia was measured by one-step qRT-PCR. Gene expression levels were normalized to the expression level of *GAPDH* mRNA. * $p < 0.05$, ** $p < 0.01$, *** $p < 0.001$, and **** $p < 0.0001$ indicate significant differences compared to normal controls. Data are presented as means \pm SDs ($n = 3$).

a suitable small animal model for the evaluation of vaccines. The findings of this study provide novel insights into HCV pathogenesis and virus-host interactions.

Materials and Methods

Animals. The tupaia used in this study were obtained from the Laboratory Animal Center at the Kunming Institute of Zoology, Chinese Academy of Sciences (Kunming, China). This study was carried out following the Guidelines for Animal Experimentation of the Japanese Association for Laboratory Animal Science and the Guide for the Care and Use of Laboratory Animals of the National Institutes of Health. All experimental protocols

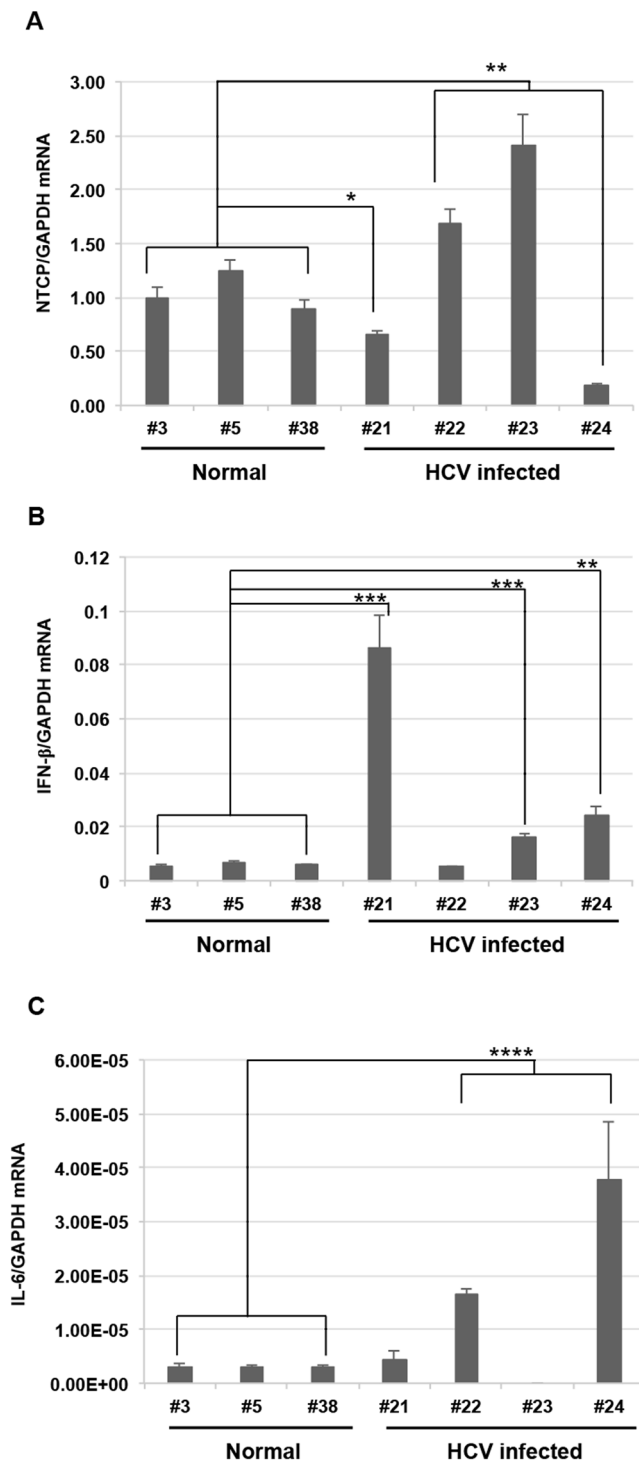


Figure 8. Changes in the expression of *NTCP* and cytokine mRNAs in HCV-infected tupaia at 41 wpi. **(A)** *NTCP*, **(B)** *IFN-β*, and **(C)** *IL-6* mRNA expression in livers of HCV-infected tupaia was measured by one-step qRT-PCR. Gene expression levels were normalized to the expression level of *GAPDH* mRNA. * $p < 0.05$, ** $p < 0.01$, *** $p < 0.001$, and **** $p < 0.0001$ indicate significant differences compared to normal controls. Data are presented as means \pm SDs ($n = 3$).

were approved by the institutional review boards of the regional ethics committees of Kagoshima University (VM15051 and VM13044).

Animals were individually housed in cages and fed a daily regimen of eggs, fruit, water, and dry mouse food. The animals were humanely handled in accordance with the Institutional Animal Care and Use Committee for Laboratory Animals.

Virus infection. All animals were found to be negative for HCV by quantitative real-time detection (RTD)-PCR before viral infection. Four adult tupaia (#21, #22, #23, and #24) were infected with HCV (genotypes 1a, 1b, 4a, and 2a [JFH1]), as described previously²⁶, and three normal tupaia (#3, #5, and #38), which were not infected with HCV, were used as controls. Briefly, tupaia (#21, #22, #23, and #24) were infected at 12 months of age under anaesthesia induced by intramuscular injection of ketamine hydrochloride and atropine at 50 mg/kg body weight prior to virus inoculation and bleeding. Inocula derived from chimeric mice were introduced twice intraperitoneally at 1.5×10^8 copies/mL for genotype 1a, 10^7 copies/mL for genotypes 1b and 4a, and 1.2×10^8 copies/mL for genotype 2a (JFH1) for tupaia #21, #22, #23, and #24, respectively.

The infected animals were bled (0.5 mL) biweekly, and sera were separated, aliquoted, and immediately used or stored at -80°C for further analysis. At 41 wpi, infected and control animals were sacrificed, and liver tissues were extracted. RNA from liver tissues was isolated using the acid guanidinium-phenol-chloroform extraction method and purified with an RNeasy Mini Kit (Qiagen, Valencia, CA, USA). For histological analysis, liver tissues were characterized by haematoxylin and eosin (H&E) or silver staining, as described previously⁴⁷.

Measurement of ALT levels and viral load. Serum ALT level was determined using a Transnase Nissui kit (Nissui Pharmaceutical Co. Ltd., Tokyo, Japan); data were standardized and represented in IU/L. RNA was isolated from sera (50 μL) using SepaGene RV-R (Sanko Junyaku Co., Ltd., Tokyo, Japan). HCV RNA levels were quantified using qRT-PCR, as reported previously⁴⁸.

Gaussia luciferase immunoprecipitation system (GLIPS) assays. To evaluate antibody levels, GLIPS assays were performed as reported previously⁴⁹, with some modifications, using SureBeads Protein G magnetic beads (Bio-Rad, Hercules, CA, USA). Briefly, the HCV core gene (1b, nucleotides 341–759), HCV NS3 gene (1b, nucleotides 3991–4753), and tupaia *DHCR24* gene (nucleotides 31–1599) were subcloned into the *Gaussia* luciferase vector (pGLIP vector)⁴⁹ and expressed in HEK293 cells with Lipofectamine LTX and Plus Reagent (Invitrogen, Carlsbad, CA, USA) according to the manufacturer's instructions. At 24–48 h after transfection, cells were lysed with *Renilla* Luciferase Assay Lysis Buffer ($1 \times$) and centrifuged at $20,380 \times g$ for 5 min at 4°C , and supernatants were collected and used immediately or stored at -80°C . The luminescence of the crude extract was measured for 10 s using the *Renilla* luciferase assay system (Promega, Madison, WI, USA) on the GloMax-Multi + Detection System (Promega).

Immunoprecipitation assays were performed in duplicate in 96-well plates, and 100-fold diluted serum (1 μL equivalent) was used. To prepare beads, 25 μL of the Protein G magnetic bead suspension was added to each well and washed with 200 μL phosphate-buffered saline (PBS) + 0.1% Tween 20 (PBS-T) three times using a DynaMag-96 Side Skirted plate (Invitrogen). Supernatants were removed using an aspirator. Next, 100 μL of diluted serum from HCV-infected or mock-infected tupaia or known antibodies (used as a positive control) of different concentrations (10, 100, or 1000 ng) was added to the beads and incubated for 30 min at room temperature on a rotator. The beads were then washed three times with PBS-T, and lysates containing corresponding antigen or negative control antigens (empty vector) of 10^7 light units were added to each well. After 1-h incubation at room temperature on a rotator, beads were washed with PBS-T at least three times. Finally, the beads were transferred with 50 μL of PBS into plates to be read, and 50 μL of *Renilla* substrate-buffer mixture ($1 \times$) was added to each well using an injector system during luminescence measurement, as stated above. The antibody titre was expressed as relative light units (RLU).

Quantification of ROS levels. Total free radicals in serum or liver samples from HCV-infected and uninfected control tupaia were measured using an OxiSelect *In Vitro* ROS/RNS Assay Kit (Cell Biolabs, Inc., San Diego, CA, USA) according to the manufacturer's protocol. Each reaction was performed in duplicate. Different concentrations of H_2O_2 were used in each reaction plate as positive controls to confirm the test conditions. Sera were diluted in PBS (1:200), and 50 μL of the diluted samples was collected into each well for the assay. For tissue lysates, 30 mg of liver tissues was homogenised using TissueLyser LT (Qiagen) in 1 mL PBS and centrifuged at $10,000 \times g$ for 5 min. The supernatant was diluted in PBS (1:100), and 50 μL of the diluted samples was used in each well for the assay. The stabilized, highly reactive 2',7'-dichlorodihydrofluorescein (DCFH) form was oxidized by ROS in the samples, and a catalyst was added to accelerate the reaction. The fluorescence of the oxidized DCFH to 2',7'-dichlorofluorescein (DCF) was proportional to the concentration of ROS in the samples. Green fluorescence was monitored at 525 nm excitation/580–640 nm emission using the GloMax-Multi + Detection System (Promega). The ROS level was expressed as relative fluorescence units (RFU).

Determination of 8-OHdG levels in genomic DNA from liver tissues. DNA was extracted from frozen liver tissues using the phenol-chloroform extraction method. The level of 8-OHdG in extracted DNA was determined using the OxiSelect Oxidative DNA Damage ELISA Kit (Cell Biolabs, Inc.) according to the manufacturer's protocol with some modifications. Briefly, 100 μg DNA was digested with 6 units of nuclease P1 for 2 h at 37°C in a final concentration of 200 nM sodium acetate (pH 5.5). Then, the DNA reaction mixture was subjected to further digestion with 2 units of alkaline phosphatase for 1 h at 37°C in a final concentration of 1M Tris (pH 7.5). Finally, the reaction mixture was centrifuged for 5 min at $6,000 \times g$ and the supernatant was used for 8-OHdG ELISA assay. Each reaction was performed in duplicate. The 8-OHdG content in unknown samples was determined by comparison with predetermined 8-OHdG standard curves.

Gene expression analysis by qRT-PCR. Tupaia TLR and cytokine mRNA expression levels were measured by qRT-PCR, as described previously⁵⁰. Primers used to detect tupaia *NTCP* gene [GenBank accession number: JQ608471] were as follows: forward primer (5'-TGTGGGCAAGAGCATCATGT-3') and reverse primer (5'-CACTGTGCATTGAGGCGAAA-3'), and the reaction conditions were similar to that used for *TLR8*⁵⁰. Tupaia *GAPDH* was used as an endogenous control for normalization of the results.

Statistical analysis. To analyse the statistical significance of antibody titres and ROS levels in animals before and after infection and to determine gene expression differences between uninfected controls and virus-infected individuals, unpaired t-tests were conducted using GraphPad software (<http://graphpad.com/quickcalcs/ttest1/>). Differences with *P* values of less than 0.05 were considered significant. All tests were two-sided.

References

- Lavanchy, D. The global burden of hepatitis C. *Liver international: official journal of the International Association for the Study of the Liver* **29**(Suppl 1), 74–81 (2009).
- Mohd Hanafiah, K., Groeger, J., Flaxman, A. D. & Wiersma, S. T. Global epidemiology of hepatitis C virus infection: new estimates of age-specific antibody to HCV seroprevalence. *Hepatology* **57**, 1333–1342 (2013).
- Horner, S. M. & Gale, M. Jr. Regulation of hepatic innate immunity by hepatitis C virus. *Nature medicine* **19**, 879–888 (2013).
- Thimme, R., Binder, M. & Bartenschlager, R. Failure of innate and adaptive immune responses in controlling hepatitis C virus infection. *FEMS microbiology reviews* **36**, 663–683 (2012).
- Cashman, S. B., Marsden, B. D. & Dustin, L. B. The Humoral Immune Response to HCV: Understanding is Key to Vaccine Development. *Frontiers in immunology* **5**, 550 (2014).
- Takeuchi, O. & Akira, S. Pattern recognition receptors and inflammation. *Cell* **140**, 805–820 (2010).
- Claro da Silva, T., Polli, J. E. & Swaan, P. W. The solute carrier family 10 (SLC10): beyond bile acid transport. *Molecular aspects of medicine* **34**, 252–269 (2013).
- Verrier, E. R. *et al.* Solute Carrier NTCP Regulates Innate Antiviral Immune Responses Targeting Hepatitis C Virus Infection of Hepatocytes. *Cell reports* **17**, 1357–1368 (2016).
- Korenaga, M. *et al.* Hepatitis C virus core protein inhibits mitochondrial electron transport and increases reactive oxygen species (ROS) production. *The Journal of biological chemistry* **280**, 37481–37488 (2005).
- Tsukiyama-Kohara, K. Role of oxidative stress in hepatocarcinogenesis induced by hepatitis C virus. *International journal of molecular sciences* **13**, 15271–15278 (2012).
- Valavanidis, A., Vlachogianni, T. & Fiotakis, C. 8-hydroxy-2'-deoxyguanosine (8-OHdG): A critical biomarker of oxidative stress and carcinogenesis. *Journal of environmental science and health. Part C, Environmental carcinogenesis & ecotoxicology reviews* **27**, 120–139 (2009).
- Waterham, H. R. *et al.* Mutations in the 3beta-hydroxysterol Delta24-reductase gene cause desmosterolosis, an autosomal recessive disorder of cholesterol biosynthesis. *American journal of human genetics* **69**, 685–694 (2001).
- Takano, T. *et al.* Augmentation of DHCR24 expression by hepatitis C virus infection facilitates viral replication in hepatocytes. *Journal of hepatology* **55**, 512–521 (2011).
- Ezzikouri, S. *et al.* Serum DHCR24 Auto-antibody as a new Biomarker for Progression of Hepatitis C. *EBioMedicine* **2**, 604–612 (2015).
- Barth, H. Hepatitis C virus: Is it time to say goodbye yet? Perspectives and challenges for the next decade. *World journal of hepatology* **7**, 725–737 (2015).
- Abdelwahab, S. F. Cellular immune response to hepatitis-C-virus in subjects without viremia or seroconversion: is it important? *Infectious agents and cancer* **11**, 23 (2016).
- Chinchilla-Lopez, P., Qi, X., Yoshida, E. M. & Mendez-Sanchez, N. The Direct-Acting Antivirals for Hepatitis C Virus and the Risk for Hepatocellular Carcinoma. *Annals of hepatology* **16**, 328–330 (2017).
- Mercer, D. F. *et al.* Hepatitis C virus replication in mice with chimeric human livers. *Nature medicine* **7**, 927–933 (2001).
- Dorner, M. *et al.* A genetically humanized mouse model for hepatitis C virus infection. *Nature* **474**, 208–211 (2011).
- Tsukiyama-Kohara, K. & Kohara, M. *Tupaia belangeri* as an experimental animal model for viral infection. *Experimental animals/Japanese Association for Laboratory Animal Science* **63**, 367–374 (2014).
- Kriegs, J. O., Churakov, G., Jurka, J., Brosius, J. & Schmitz, J. Evolutionary history of 7SL RNA-derived SINEs in Supraprimates. *Trends in genetics: TIG* **23**, 158–161 (2007).
- Fan, Y. *et al.* Genome of the Chinese tree shrew. *Nature communications* **4**, 1426 (2013).
- Yang, C. *et al.* Chronic hepatitis B virus infection and occurrence of hepatocellular carcinoma in tree shrews (*Tupaia belangeri chinensis*). *Virology journal* **12**, 26 (2015).
- Sanada, T. *et al.* Property of hepatitis B virus replication in *Tupaia belangeri* hepatocytes. *Biochemical and biophysical research communications* **469**, 229–235 (2016).
- Xu, X., Chen, H., Cao, X. & Ben, K. Efficient infection of tree shrew (*Tupaia belangeri*) with hepatitis C virus grown in cell culture or from patient plasma. *The Journal of general virology* **88**, 2504–2512 (2007).
- Amako, Y. *et al.* Pathogenesis of hepatitis C virus infection in *Tupaia belangeri*. *Journal of virology* **84**, 303–311 (2010).
- Yu, W. *et al.* Characterization of hepatitis E virus infection in tree shrew (*Tupaia belangeri chinensis*). *BMC infectious diseases* **16**, 80 (2016).
- De Maria, N. *et al.* Association between reactive oxygen species and disease activity in chronic hepatitis C. *Free radical biology & medicine* **21**, 291–295 (1996).
- Valgimigli, L., Valgimigli, M., Gaiani, S., Pedulli, G. F. & Bolondi, L. Measurement of oxidative stress in human liver by EPR spin-probe technique. *Free radical research* **33**, 167–178 (2000).
- Valgimigli, M. *et al.* Oxidative stress EPR measurement in human liver by radical-probe technique. Correlation with etiology, histology and cell proliferation. *Free radical research* **36**, 939–948 (2002).
- Mahmood, S. *et al.* Immunohistochemical evaluation of oxidative stress markers in chronic hepatitis C. *Antioxidants & redox signaling* **6**, 19–24 (2004).
- Fujita, N., Kaito, M., Tanaka, H., Horiike, S. & Adachi, Y. Reduction of serum HCV RNA titer by bezafibrate therapy in patients with chronic hepatitis C. *The American journal of gastroenterology* **99**, 2280 (2004).
- Saito, M., Kohara, M. & Tsukiyama-Kohara, K. Hepatitis C virus promotes expression of the 3beta-hydroxysterol delta24-reductase through Sp1. *Journal of medical virology* **84**, 733–746 (2012).
- Ishii, K. *et al.* [Characterization of antibodies against core, NS3, NS4, NS5 region of hepatitis C virus in patients with hepatitis C]. *Rinsho byori. The Japanese journal of clinical pathology* **45**, 1156–1162 (1997).
- Hoare, M. *et al.* Histological changes in HCV antibody-positive, HCV RNA-negative subjects suggest persistent virus infection. *Hepatology* **48**, 1737–1745 (2008).
- Kawai, T. & Akira, S. The role of pattern-recognition receptors in innate immunity: update on Toll-like receptors. *Nature immunology* **11**, 373–384 (2010).
- Akira, S., Uematsu, S. & Takeuchi, O. Pathogen recognition and innate immunity. *Cell* **124**, 783–801 (2006).
- Yang, D. R. & Zhu, H. Z. Hepatitis C virus and antiviral innate immunity: who wins at tug-of-war? *World journal of gastroenterology: WJG* **21**, 3786–3800 (2015).
- Metz, P., Reuter, A., Bender, S. & Bartenschlager, R. Interferon-stimulated genes and their role in controlling hepatitis C virus. *Journal of hepatology* **59**, 1331–1341 (2013).
- Lee, J. *et al.* TNF-alpha Induced by Hepatitis C Virus via TLR7 and TLR8 in Hepatocytes Supports Interferon Signaling via an Autocrine Mechanism. *PLoS pathogens* **11**, e1004937 (2015).

41. Foy, E. *et al.* Control of antiviral defenses through hepatitis C virus disruption of retinoic acid-inducible gene-1 signaling. *Proceedings of the National Academy of Sciences of the United States of America* **102**, 2986–2991 (2005).
42. Sklan, E. H., Charuorn, P., Pang, P. S. & Glenn, J. S. Mechanisms of HCV survival in the host. *Nature reviews. Gastroenterology & hepatology* **6**, 217–227 (2009).
43. Li, K. *et al.* Immune evasion by hepatitis C virus NS3/4A protease-mediated cleavage of the Toll-like receptor 3 adaptor protein TRIF. *Proceedings of the National Academy of Sciences of the United States of America* **102**, 2992–2997 (2005).
44. Bode, J. G. *et al.* IFN-alpha antagonistic activity of HCV core protein involves induction of suppressor of cytokine signaling-3. *FASEB journal: official publication of the Federation of American Societies for Experimental Biology* **17**, 488–490 (2003).
45. Polyak, S. J. *et al.* Hepatitis C virus nonstructural 5A protein induces interleukin-8, leading to partial inhibition of the interferon-induced antiviral response. *Journal of virology* **75**, 6095–6106 (2001).
46. Rehermann, B. Hepatitis C virus versus innate and adaptive immune responses: a tale of coevolution and coexistence. *The Journal of clinical investigation* **119**, 1745–1754 (2009).
47. Sekiguchi, S. *et al.* Immunization with a recombinant vaccinia virus that encodes nonstructural proteins of the hepatitis C virus suppresses viral protein levels in mouse liver. *PLoS one* **7**, e51656 (2012).
48. Takeuchi, T. *et al.* Real-time detection system for quantification of hepatitis C virus genome. *Gastroenterology* **116**, 636–642 (1999).
49. Matsuu, A. *et al.* Genetic and serological surveillance for non-primate hepacivirus in horses in Japan. *Veterinary microbiology* **179**, 219–227 (2015).
50. Kayesh, M. E. H. *et al.* Susceptibility and initial immune response of Tupaia belangeri cells to dengue virus infection. *Infection, genetics and evolution: journal of molecular epidemiology and evolutionary genetics in infectious diseases* **51**, 203–210 (2017).

Acknowledgements

This work was supported by grants from the Japan Agency for Medical Research and Development (AMED, J15000952, 16fk0210108s0201), the Tokyo Metropolitan Government; the Ministry of Health, Labour and Welfare of Japan; and the Ministry of Education, Culture, Sports, Science and Technology of Japan (25.03079). S.E. is supported by a Japan Society for the Promotion of Science (JSPS) Fellowship for Foreign Researchers (P13079). We would like to thank Dr Horie for supplying the pGLIP vector and Mr Haraguchi, Ms Matsuyama, Mr Kanda, Ms Nakagawa, Mr Okuya, Mr Ueno, Mr Handa, Dr Ozawa, and Dr Chimene for their assistance with animal care.

Author Contributions

M.E.H.K., S.E., H.C., K.R., and B.K. performed experiments; A.M. supervised GLIPS assays; N.M. performed pathological analyses; T.S., Y.H., and T.H. performed silver staining and updated H&E analysis; and M.E.H.K., S.E., M.K., and K.T.-K. designed and performed experiments and wrote the manuscript.

Additional Information

Supplementary information accompanies this paper at doi:[10.1038/s41598-017-10329-7](https://doi.org/10.1038/s41598-017-10329-7)

Competing Interests: The authors declare that they have no competing interests.

Publisher's note: Springer Nature remains neutral with regard to jurisdictional claims in published maps and institutional affiliations.



Open Access This article is licensed under a Creative Commons Attribution 4.0 International License, which permits use, sharing, adaptation, distribution and reproduction in any medium or format, as long as you give appropriate credit to the original author(s) and the source, provide a link to the Creative Commons license, and indicate if changes were made. The images or other third party material in this article are included in the article's Creative Commons license, unless indicated otherwise in a credit line to the material. If material is not included in the article's Creative Commons license and your intended use is not permitted by statutory regulation or exceeds the permitted use, you will need to obtain permission directly from the copyright holder. To view a copy of this license, visit <http://creativecommons.org/licenses/by/4.0/>.

© The Author(s) 2017